

1 **SUPPLEMENTARY MATERIALS: AN ALGORITHM SOLVING**
2 **COMPRESSIVE SENSING PROBLEMS BASED ON MAXIMAL**
3 **MONOTONE OPERATORS***

4 YOHANN TENDERO^T, IGOR CIRIL[‡], JÉRÔME DARBON[§], AND SUSANA SERNA[¶]

5 **SM1. Comparison of solutions of AISS, LARS, SPGL1, SeDuMi and**
6 **algorithm 2.1 in terms of ℓ^1 norm.** We wish to compare the ℓ^1 -based methods
7 considered in this paper, i.e., AISS [SM7], LARS [SM18], SPGL1 [SM40, SM41],
8 SeDuMi [SM38] and algorithm 2.1 beyond the “probability of success” (4.1). Since
9 the minimizer(s) to (P_{ℓ^1}) may not be unique we compare the ℓ^1 norms of the solutions
10 produced by the above algorithms. To so do, let \mathbf{b}^i denote the i -th observed vector
11 and let \mathbf{u}_k^i denote the i -th output of the algorithm k . We compare the algorithms
12 by computing the solution with the smallest ℓ^1 -norm among feasible solutions. This
13 yields to the following formula to compute the score S_k of algorithm k with

14 (SM1.1)
$$S_k := \frac{1}{\# \text{ of tests}} \sum_i \mathbb{1}_{\{\|A\mathbf{u}_k^i - \mathbf{b}\|_{\ell^2} \leq \varepsilon\}}(i) \mathbb{1}_{\{\|\mathbf{u}_k^i\|_{\ell^1} = \min_k \|\mathbf{u}_k^i\|_{\ell^1}\}}(i),$$

15 where, as usual, $\varepsilon := 1e - 10$. The results of (SM1.1) applied to the above algorithms
16 are depicted in Figure SM1. From this figure, we observed that algorithm 2.1 the one
17 with highest score.

18 **SM2. Extension for the noisy case.** For applications where the observed
19 data \mathbf{b} is corrupted by a random Gaussian perturbation one is often interested in the
20 following optimization problem

21
$$\begin{cases} \inf_{\mathbf{u} \in \mathbb{R}^n} & \|\mathbf{u}\|_{\ell^1} \\ \text{s.t.} & \|A\mathbf{u} - \mathbf{b}\|_{\ell^2} \leq \epsilon \end{cases}$$

22 that can equivalently be formulated as follows for all $\epsilon \geq 0$

23 (SM2.1)
$$\begin{cases} \inf_{\mathbf{e} \in \mathbb{R}^m} & G(\mathbf{e}) \\ \text{s.t.} & \|\mathbf{e}\|_{\ell^2} \leq \epsilon, \end{cases}$$

24 where

25 (SM2.2)
$$G(\mathbf{e}) := \inf_{\substack{\mathbf{u} \in \mathbb{R}^n \\ A\mathbf{u} - \mathbf{b} = \mathbf{e}}} \|\mathbf{u}\|_{\ell^1}.$$

A Lagrangian-based approach can be used for solving SM2.1. Consider the Lagrangian
 $\mathcal{L}_G : \mathbb{R}^m \times [0, +\infty) \rightarrow \mathbb{R} \cup \{+\infty\}$ defined as

$$\mathcal{L}_G(\mathbf{e}, \mu) = G(\mathbf{e}) + \mu(\|\mathbf{e}\|_{\ell^2} - \epsilon).$$

*Submitted to the editors DATE. A preliminary version of the work is [SM13].

Funding: Research of J. Darbon has been supported by the National Science Foundation under Grant No. NSF-1820821.

^TDR2I, Institut Polytechnique des Sciences Avancées, 94200, Ivry-sur-Seine, France yohann.tendero@ipsa.fr.

[‡]DR2I, Institut Polytechnique des Sciences Avancées, 94200, Ivry-sur-Seine, France igor.ciril@ipsa.fr.

[§]Division of Applied Mathematics, Brown University, Providence, RI 02912, USA

[¶]Departament de Matemàtiques, Universitat Autònoma de Barcelona, Bellaterra, Barcelona, Spain susana.serna@uab.cat

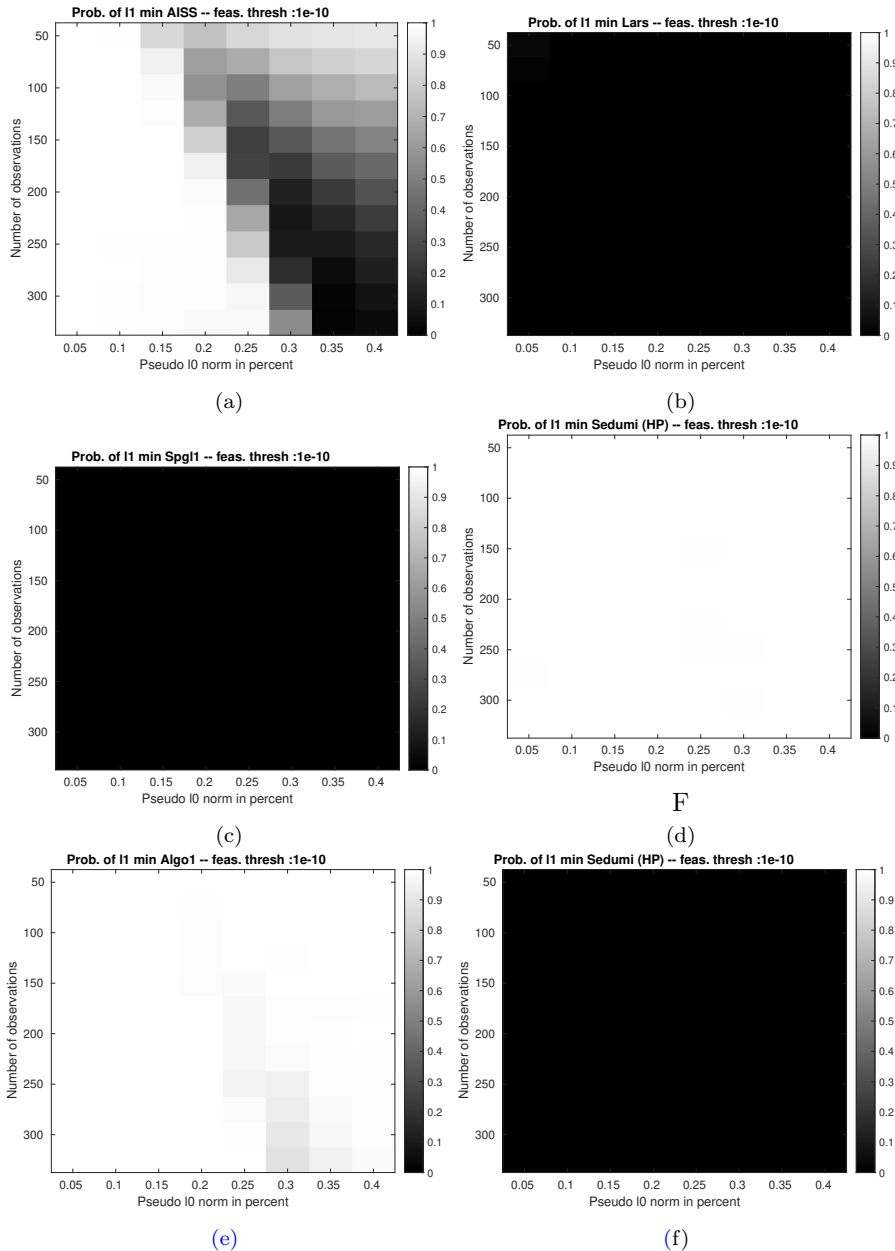


FIG. SM1. Algorithms ranking: l^1 -minimization. This figures compares the quality of produced solutions by the considered algorithms using (SM1.1). A white color means a high score and a black color a low score. Panel (a): AISS [SM7], panel (b): LARS [SM18], panel (c): SPGL1 [SM40, SM41], panel (d): SeDuMi (SP) [SM38] panel (e): algorithm 2.1, panel (f): SeDuMi (HP) [SM38].

27 Existence of a saddle point of this Lagrangian easily follows from the mini-max the-
 28 orem [SM3, chap. 6] combined with our assumptions. We can proceed as follows
 29 to find a saddle-point of the Lagrangian \mathcal{L}_G . We can minimize $\mathcal{L}_G(\cdot, \mu)$ when μ is
 30 fixed using a black-box method as described in [SM1, section 8.3.1] (see below for
 31 a justification that the black-box can be computed using our algorithm). Then, we

32 can perform a bitonic-search on $\mathcal{L}_G(e, \cdot)$ to find the optimal Lagrange multiplier. We
 33 intend to program and test this approach and to provide details in our next paper.

34 We now briefly justify how to implement the black-box for G using our proposed
 35 algorithm. Following [SM1, section 8.3.1], a black-box for G , given $e \in \mathbb{R}^m$, consists
 36 of computing $G(e)$ and $s \in \partial G(e)$. We now explain how to compute s using our
 37 proposed algorithm. Define the Lagrangian $\mathcal{L}_e : \mathbb{R}^n \times \mathbb{R}^m \rightarrow \mathbb{R}$ given by

38 (SM2.3)
$$\mathcal{L}_e(\mathbf{u}, \boldsymbol{\lambda}) := J(\mathbf{u}) + \langle \boldsymbol{\lambda}, A\mathbf{u} \rangle + \langle \boldsymbol{\lambda}, -\mathbf{b} \rangle + \langle \boldsymbol{\lambda}, -\mathbf{e} \rangle,$$

39 we immediately obtain for all $e \in \mathbb{R}^m$

40 (SM2.4)
$$G(e) = - \inf_{\boldsymbol{\lambda} \in \mathbb{R}^m} \left\{ - \inf_{\mathbf{u} \in \mathbb{R}^n} \mathcal{L}_e(\mathbf{u}, \boldsymbol{\lambda}) \right\} = - \inf_{\boldsymbol{\lambda} \in \mathbb{R}^m} \{g(\boldsymbol{\lambda}) - \langle \boldsymbol{\lambda}, -\mathbf{e} \rangle\} = g^*(-e).$$

42 Consequently, combining (SM2.3)-(SM2.4) and [SM4, prop. 11.3 p. 476] we have

43 (SM2.5)
$$\partial G(e) = \partial g^*(-e) = \arg \min_{\boldsymbol{\lambda} \in \mathbb{R}^m} \{g(\boldsymbol{\lambda}) - \langle \boldsymbol{\lambda}, -\mathbf{e} \rangle\}.$$

44 We immediately notice that the problem in (SM2.5) has the same form as the dual
 45 problem (D_{ℓ^1}) that we considered in this paper. Our algorithm allows us to efficiently
 46 compute an optimal $\bar{\boldsymbol{\lambda}}$ up to the machine precision by running our algorithm on the
 47 input vector $\mathbf{b} + \mathbf{e}$.

48 **SM3. Extension to inequality constraints.** Note that our proposed ap-
 49 proach can be extended to handle inequality constraints. This is easily achieved
 50 using well-known equivalent reformulation of optimization problems (see e.g., [SM2,
 51 section 4.1.3]). Let us first consider the case of an inequality constraint that reads
 52 $\langle a, u \rangle - b \leq \epsilon$ where $\epsilon \in [0, +\infty)$. The above inequality is equivalent to the following
 53 equality constraint $\langle a, u \rangle - b + \gamma = \epsilon$ where $\gamma \geq 0$. Therefore any affine inequal-
 54 ity constraints of the form can be mapped to an equality constraints using an extra
 55 variable. The above procedure trivially extends to any finite number of constraints
 56 that read $\langle a_i, u \rangle - b \leq \epsilon$ with $i = 1, \dots, M$ where $M \in \mathbb{N}$. As an application of the
 57 above procedure, we can for instance deal with constraints that read $\|Au - b\|_{\ell^\infty} \leq \epsilon$
 58 or $\|Au - b\|_{\ell^1} \leq \epsilon$. Note that $\|\cdot\|_\infty$ or $\|\cdot\|_1$ norms can be replaced by any polyhedral
 59 norms (that can include weights) using the same procedure.

60 **SM4. Additional Experiments.** This section proposes an empirical evalua-
 61 tion of: OMP [SM35], CoSamp [SM33], GISS [SM32]. Note that OMP, CoSamp and
 62 GISS are greedy-based numerical algorithms while LARS, SPGL1, AISS and **Algo-**
 63 **gorithm 2.1** developed in the paper corresponding to this supplementary material are
 64 ℓ^1 -based numerical algorithms. (Comparisons between LARS, SPGL1, AISS and **Al-**
 65 **gorithm 2.1** are in section 4).

66 These methods are compared in terms of a “probability of success”, as in section 4.
 67 The experimental setup is the same as in section 4. The implementation of CoSamp
 68 and OMP we used are due to S. Becker (code updated on Dec 12th, 2012) and can
 69 be found on Mathworks file exchange¹. The implementation of GISS we used are
 70 the ones given by the authors of [SM7, SM32]. Note that the implementation of
 71 CoSamp requires an estimate of the sparsity. In all the experiments we used an
 72 oracle for CoSamp, i.e., provided the exact sparsity of the source element. Default
 73 parameters have been used for all methods. We now give the criteria used for the

¹ <https://fr.mathworks.com/matlabcentral/fileexchange/32402-cosamp-and-omp-for-sparse-recovery>

74 numerical comparisons of these numerical algorithms. We recall that a reconstruction
 75 is *a success* if the relative error satisfies $\frac{\|\mathbf{u}-\mathbf{u}_{est}\|_{\ell^2}}{\|\mathbf{u}\|_{\ell^2}} < \varepsilon$, where $\varepsilon = 10^{-10}$ or $\varepsilon = 10^{-4}$
 76 as in section 4. As in section 4 equation (4.1), the empirical probability of success is
 77 given by

$$78 \quad P_{(m,s)} := \frac{1}{\# \text{ of tests}} \sum_i \mathbb{1}_{\left\{ \frac{\|\mathbf{u}^i - \mathbf{u}_{est}^i\|_{\ell^2}}{\|\mathbf{u}^i\|_{\ell^2}} < \varepsilon \right\}}(i).$$

79 Each method is tested on the same data by using the same random seed. We first
 80 consider $\varepsilon = 10^{-10}$. Figure SM2 depicts the empirical probability of success (4.1) for
 81 OMP, CoSamp, and GISS algorithms. As in section 4, we consider the difference of
 82 probability of success between Algorithm 2.1 and all other methods

$$83 \quad D_{(m,s)} := P_{(m,s)}^{Algorithm\ 2.1} - P_{(m,s)},$$

84 where $m \in M$, $s \in S$, $P_{(m,s)}^{Algorithm\ 2.1}$ (resp. $P_{(m,s)}$) denotes the quantity (4.1) obtained
 85 with Algorithm 2.1 (resp. OMP, CoSamp or GISS). Note that a positive (negative)
 86 value in (4.2) means that Algorithm 2.1 achieves a higher (lower) probability of success
 87 than the compared algorithm. These differences of probability of success are depicted
 88 in figure SM3. It is easily seen that OMP and CoSamp succeed at retrieving the source
 89 signal with a probability of approximately 80% for a larger set of parameters than
 90 any other method. However, they produce correct results with a probability of nearly
 91 100% for a much smaller set of parameters than AISS, GISS, and Algorithm 2.1
 92 (see section 4). We also deduce from figure SM3 that Algorithm 2.1 always achieves
 93 a higher probability of success than GISS. An overview of the main similarities and
 94 differences between OMP [SM35], CoSamp [SM33], GISS [SM32] and Algorithm 2.1
 95 are given in table SM1. In table SM1, we give the empirical probability that at least
 96 $x\%$ of signals are successfully reconstructed for all methods. This statistical indicator
 97 is defined as in section 4

$$98 \quad (SM4.1) \quad P_{\geq x} = \frac{\# \{(m,s) \in M \times S : P_{(m,s)} \geq x\}}{\#M \cdot \#S},$$

99 where $P_{(m,s)}$ is defined by (4.1) and $\#$ denotes the cardinality of a set. We now report
 100 results concerning the number of iterations needed to achieve convergence.

101 Figure SM4 gives the average number of iterations needed by the considered algo-
 102 rithms. OMP and GISS are much faster than Algorithm 2.1 with a maximal average
 103 number of iterations of (about) 250 and 300 respectively. The maximal average num-
 104 ber of iterations needed by CoSamp fluctuates more depending on the sparsity. For
 105 CoSamp it remains below 300 for most experiments though and the maximal average
 106 number of iterations is bounded from above by 1,000.

107 Figure SM5 depicts the empirical probability of success (4.1) for OMP, CoSamp,
 108 and GISS algorithms. Figure SM6 depicts the differences of probability of success.

109

REFERENCES

- 110 [SM1] J.-F. BONNANS, J. GILBERT, C. LEMARECHAL, AND C. SAGASTIZABAL, *Numerical Optimization*, Springer Berlin Heidelberg, 2006.
 111 [SM2] S. P. BOYD AND L. VANDENBERGHE, *Convex Optimization*, Cambridge University Press,
 112 2014, <https://doi.org/10.1017/CBO9780511804441>, <https://web.stanford.edu/%7Eboyd/cvxbook/>.
 113
 114

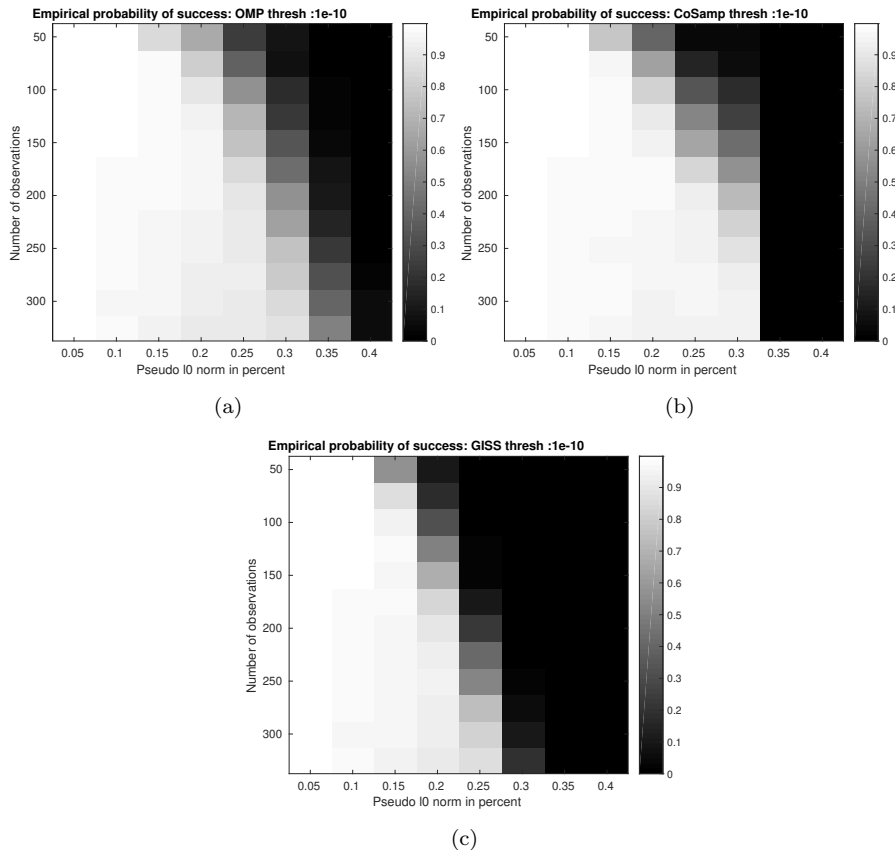


FIG. SM2. Empirical probability of success (4.1), with $\varepsilon = 10^{-10}$. Panel (a): OMP [SM35], panel (b): CoSamp [SM33] and panel (c): GISS [SM32]. The non-zero entries of the source element \mathbf{u} are drawn from a uniform distribution on $[-1, 1]$. The entries in A are drawn from i.i.d. realizations of a Gaussian distribution.

TABLE SM1

Main assumption and statistical indicator of “success” for OMP, CoSamp and GISS methods. The numbers without parentheses correspond to $\varepsilon = 10^{-10}$ and those between parentheses correspond to $\varepsilon = 10^{-4}$. Below, E.R.C. stands for exact recovery condition see, e.g., [SM35], R.I.C. stands for restricted isometry constant see, e.g., [SM33].

Algorithm	OMP [SM35]	CoSamp [SM33]	GISS [SM32]
Assumption(s): A/b	E.R.C.	R.I.C.	E.R.C.
$P_{\geq 0.9}$ (SM4.1)	0.5104 (0.5417)	0.5521 (0.5625)	0.4063 (0.4167)
$P_{\geq 0.95}$ (SM4.1)	0.3854 (0.4479)	0.4583 (0.5208)	0.3333 (0.3542)
$P_{\geq 0.99}$ (SM4.1)	0.1042 (0.1354)	0.1250 (0.1458)	0.1042 (0.1354)
$P_{\geq 0.999}$ (SM4.1)	0 (0)	0 (0)	0 (0)
$P_{\geq 1}$ (SM4.1)	0 (0)	0 (0)	0 (0)

115 [SM3] I. EKELAND AND R. TEMAM, *Convex analysis and variational problems*, SIAM, 1999.
 116 [SM4] R. T. ROCKAFELLAR AND R. J.-B. WETS, *Variational Analysis*, Grundlehren der mathematischen Wissenschaften, Springer Berlin Heidelberg, 2009.
 117

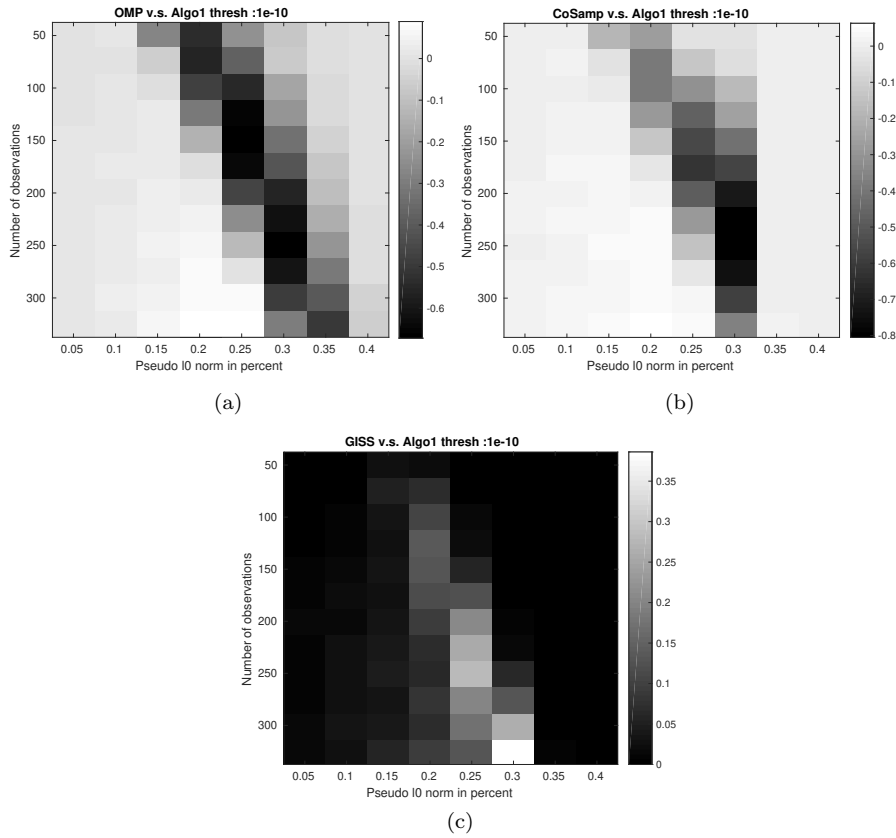


FIG. SM3. Differences of probability of success (4.2), with $\varepsilon = 10^{-10}$. Panel (a): *Algorithm 2.1-OMP* [SM35], panel (b): *Algorithm 2.1-CoSamp* [SM33] and panel (c): *Algorithm 2.1-GISS* [SM32]. A positive value indicates that *Algorithm 2.1* achieves a higher probability of success than the considered method, a negative value the contrary.

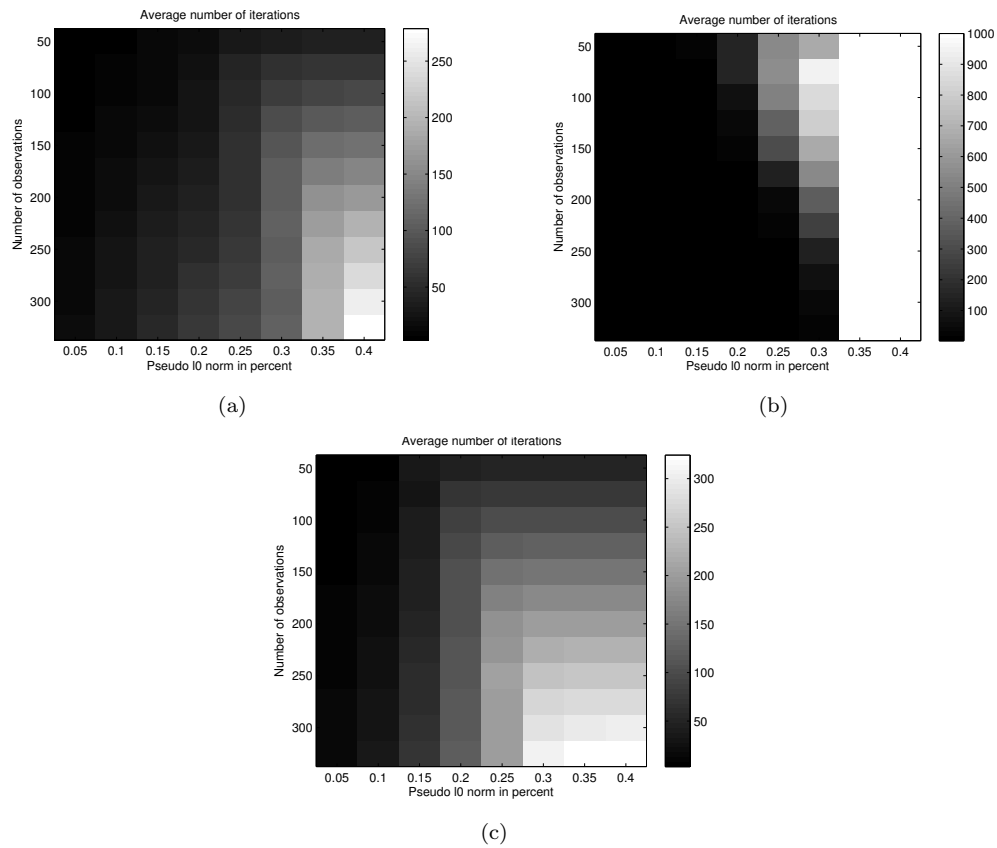


FIG. SM4. Average number of iterations. Panel (a): OMP [SM35], panel (b): CoSamp [SM33] and panel (c): GISS [SM32].

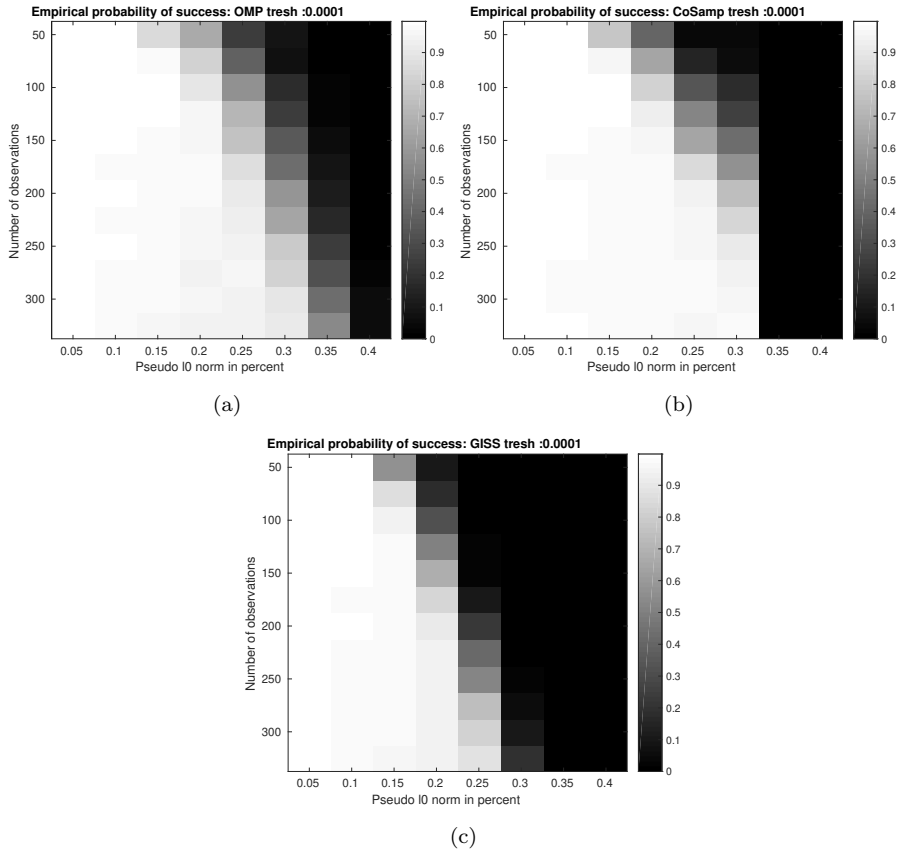


FIG. SM5. Empirical probability of success (4.1), with $\varepsilon = 10^{-4}$. Panel (a): OMP [SM35], panel (b): CoSamp [SM33] and panel (c): GISS [SM32]. The non-zero entries of the source element \mathbf{u} are drawn from a uniform distribution on $[-1, 1]$. The entries in A are drawn from *i.i.d.* realizations of a Gaussian distribution.

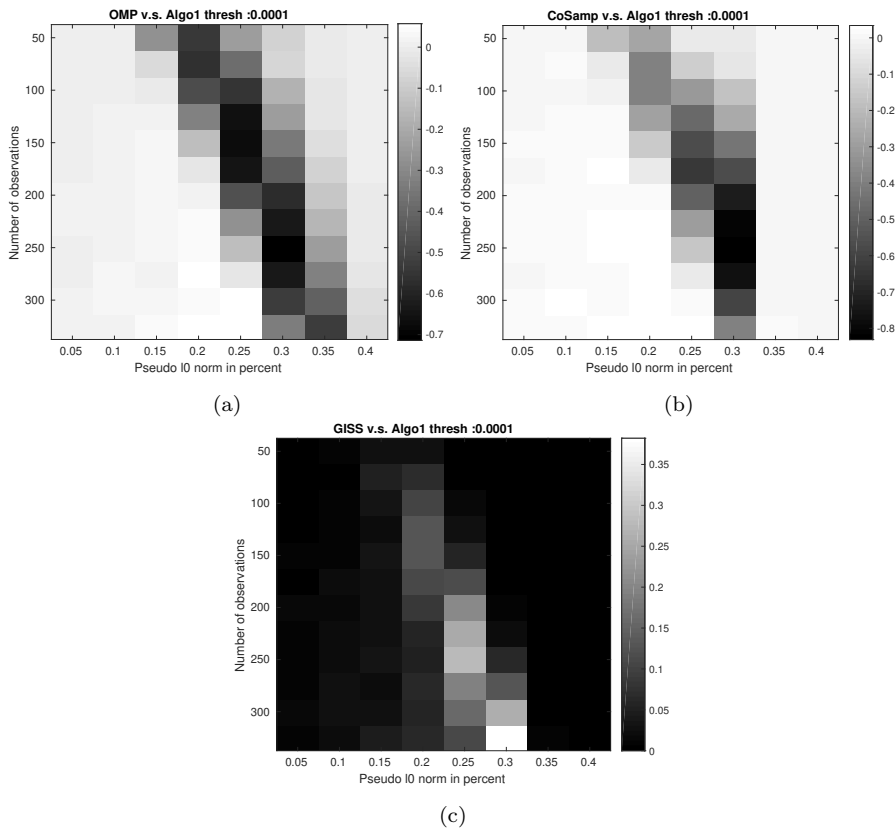


FIG. SM6. Differences of probability of success (4.2), with $\varepsilon = 10^{-4}$. Panel (a): Algorithm 2.1-OMP [SM35], panel (b): Algorithm 2.1-CoSamp [SM33] and panel (c): Algorithm 2.1-GISS [SM32]. A positive value indicates that Algorithm 2.1 achieves a higher probability of success than the considered method, a negative value the contrary.